
Quaternion Knowledge Graph Embedding

Shuai Zhang*

University of New South Wales
Sydney, Australia
shuai.zhang@student.unsw.edu.au

Yi Tay*

Nanyang Technological University
Nanyang Avenue, Singapore
ytay017@e.ntu.edu.sg

Lina Yao

University of New South Wales
Sydney, Australia
lina.yao@unsw.edu.au

Qi Liu

University of Oxford
Oxford, UK
qiliu@u.nus.edu

Abstract

Complex-valued representations have demonstrated promising results on modeling relational data, i.e., knowledge graphs. This paper proposes a new knowledge graph embedding method. More concretely, we move beyond standard complex representations, adopting expressive hypercomplex representations for learning representations of entities and relations. Hypercomplex embeddings, or Quaternion embeddings (**QuatE**), are complex valued embeddings with three imaginary components. Different from standard complex (Hermitian) inner product, latent inter-dependencies (between all components) are aptly captured via the Hamilton product in Quaternion space, encouraging a more efficient and expressive representation learning process. Moreover, Quaternions are intuitively desirable for smooth and pure rotation in vector space, preventing noise from sheer/scaling operators. Finally, Quaternion inductive biases enjoy and satisfy the key desiderata of relational representation learning (i.e., modeling symmetry, anti-symmetry and inversion). Experimental results demonstrate that QuatE achieves state-of-the-art performance on four well-established knowledge graph completion benchmarks.

1 Introduction

Knowledge graphs (KGs) live at the heart of many semantic applications. KGs provide an effective way to understanding how entities are connected, not only enabling powerful relational reasoning but also the ability to learn structural representations. As such, reasoning with KGs have been an extremely productive research direction, with many innovations leading to improvements to many downstream applications (e.g., question answering, search, natural language processing etc.). To this end, representation learning of entities and relations in a knowledge graph have been an incredibly promising direction.

Not unsurprisingly, it turns out that the complex space \mathbb{C} serves as a highly effective inductive bias for learning KG embeddings, largely owing to its intrinsic asymmetrical properties. This is demonstrated by the ComplEx embedding method which composes relational triplets with the asymmetrical Hermitian product. In this paper, we move beyond complex representations, exploring Hypercomplex space as an inductive bias for learning KG embeddings. More concretely, we propose Quaternion embeddings (QuatE), a novel representation learning method that achieves state-of-the-art performance on all well-established KG embedding benchmarks.

*Equal contribution.

Hypercomplex Quaternion representations are complex spaces \mathbb{H} with three imaginary components i, j, k , as opposed to the standard complex space \mathbb{C} with a single real component r and imaginary component i . There are numerous benefits for this formulation. Firstly, the Hamilton operator provides a greater extent of expressiveness compared to the complex Hermitian operator and the real inner product. Even at equal parameterization, the Hamilton operator forges inter-latent interactions between all of r, i, j, k , resulting in a highly expressive model. This draws similarities with methods such as Capsule networks [Sabour et al., 2017]. Secondly, Quaternion representations are highly desirable for parameterizing smooth rotation and spatial transformations in vector space. Moreover, they are generally considered robust to sheer/scaling noise and perturbations (i.e., numerically stable rotations) and avoid the problem of Gimbal locks. Lastly, our QuatE framework subsumes the ComplEx method, concurrently inheriting its attractive properties such as its ability to model symmetry, anti-symmetry and inversion.

In our proposed QuatE (Quaternion embeddings of Knowledge Graphs), we propose a new scoring function and model that learns a relational rotation of the head entity Q_h in Quaternion space \mathbb{H} . This is followed by a component-wise multiplication with the tail entity Q_t . Experimental results on KB completion tasks demonstrate that our proposed QuatE model substantially outperforms its complex-valued counterpart (i.e., ComplEx) while maintaining equal parameterization.

2 Related Work

Knowledge graph embedding has attracted intense research focus in recent years and a myriad of embedding methodologies have been proposed. The key differentiator in these these methods mainly lies in the composition over head, relation and tail entities, i.e., the scoring function.

Translational methods that interpret relation vectors as translations in vector space are a popular choice of scoring functions, i.e., $head + relation \approx tail$, as popularized by TransE [Bordes et al., 2013]. Subsequently, a number of models aim to improve TransE. TransH [Wang et al., 2014] introduces relation-specific hyperplanes with a normal vector. TransR [Lin et al., 2015] further introduces relation-specific spaces by modelling entities and relations in distinct spaces with a shared projection matrix. TransD [Ji et al., 2015] uses independent projection vectors for each entity and relation and could reduce the amount of calculation of TransR. TorusE [Ebisu and Ichise, 2018] defines embeddings and distance function in a compact Lie group, torus and shows better accuracy and scalability than TransE. The recent state-of-the-art, RotatE [Sun et al., 2019] proposed a rotation based translational method with complex number embeddings.

On the other hand, semantic matching models include bilinear models such as RESCAL [Nickel et al., 2011], DistMult [Yang et al., 2014], HolE [Nickel et al., 2016] and ComplEx [Trouillon et al., 2016] and neural network-based models. These methods measure plausibility by matching latent semantics of entities and relations. In RESCAL, each relation is represented with a square matrix, while DistMult replace it with a diagonal matrix in order to reduce the complexity. Simple [Kazemi and Poole, 2018] is also a simple yet effective bilinear approach for knowledge graph embedding. HolE explores the holographic reduced representations and makes use of circular correlation to capture rich interactions between entities. ComplEx embeds entities and relations in complex space and utilizes Hermitian product to model the antisymmetric patterns, which have shown to be immensely helpful in learning KG representations. The scoring function of ComplEx is isomorphic to that of HolE [Trouillon and Nickel, 2017]. Neural networks based methods have also been adopted, e.g., Neural Tensor Network [Socher et al., 2013] and ER-MLP [Dong et al., 2014] are two representative neural network based methodologies. More recently, convolution neural networks [Dettmers et al., 2018], graph convolutional networks [Schlichtkrull et al., 2018], deep memory networks [Wang et al., 2018] also show promising performance on this task.

Quaternion is a hypercomplex number systems firstly described by Hamilton [Hamilton, 1844] with applications in wide variety of areas including astronautics, robotics, computer visualisation, animation and special effects in movies, navigation. Lately, Quaternions have attracted attention in the field of machine learning. Quaternion recurrent neural networks (QRNNs) obtain better performance with fewer number of free parameters than traditional RNNs on the phoneme recognition task. Quaternion representations are also useful for enhancing the performance of convolutional neural networks on multiple tasks such as automatic speech recognition [Parcollet et al.] and image classification [Gaudet and Maida, 2018, Parcollet et al., 2018a]. Quaternion multiplayer perceptron [Parcollet et al., 2016]

and Quaternion autoencoders [Parcollet et al., 2017] also outperform standard MLP and autoencoder. In a nutshell, the major motivation behind these models is that Quaternions enables the neural networks to code latent inter- and intra-dependencies between multidimensional input features, thus, leading to better representation capability.

Our method takes the advantages (i.e., its geometrical meaning and rich representation capability, etc.) of Quaternion representations to enable rich and expressive semantic matching of entities and relations.

3 Method

We firstly introduce the Hamilton’s Quaternions and then detail the proposed method. Afterwards, we discuss the model properties and comparisons to other embedding methods.

3.1 Hamilton’s Quaternions

Quaternion [Hamilton, 1844] is a class of hypercomplex number systems which extends the complex number to four-dimensional space. It consists of one real component and three imaginary components and is defined as follows:

$$Q = a + b\mathbf{i} + c\mathbf{j} + d\mathbf{k} \quad (1)$$

where a, b, c, d are real numbers and $\mathbf{i}, \mathbf{j}, \mathbf{k}$ are imaginary units. These three imaginary units are all square roots of -1 and satisfy the following Hamilton’s rule:

$$\mathbf{i}^2 = \mathbf{j}^2 = \mathbf{k}^2 = \mathbf{ijk} = -1 \quad (2)$$

We can also derive some other relationships from this rule, such as: $\mathbf{ij} = \mathbf{k}, \mathbf{ji} = -\mathbf{k}, \mathbf{jk} = \mathbf{i}, \mathbf{ki} = \mathbf{j}, \mathbf{kj} = -\mathbf{i}$ and $\mathbf{ik} = -\mathbf{j}$. Apparently, the multiplication between imaginary units is non-commutative. Spatial rotations can be modelled with this definition. Some common operations of Quaternions algebra \mathbb{H} are introduced as follows:

- **Conjugate.** The conjugate of Quaternion Q is: $\bar{Q} = a - b\mathbf{i} - c\mathbf{j} - d\mathbf{k}$.
- **Norm.** The norm of Quaternion is defined as: $|Q| = \sqrt{a^2 + b^2 + c^2 + d^2}$.
- **Dot Product.** Similar to vector dot-products, we can also compute the dot product between two Quaternions (i.e., $Q_1 = a_1 + b_1\mathbf{i} + c_1\mathbf{j} + d_1\mathbf{k}$ and $Q_2 = a_2 + b_2\mathbf{i} + c_2\mathbf{j} + d_2\mathbf{k}$) by multiplying the corresponding scalar parts and summing the results. That is:

$$Q_1 \cdot Q_2 = a_1a_2 + b_1b_2 + c_1c_2 + d_1d_2 \quad (3)$$

- **Hamilton Product.** Hamilton product is composed of all the standard multiplications of factors in Quaternions and follows the distributive law. Thus, the Hamilton product between two Quaternions are defined as:

$$Q_1 \otimes Q_2 = (a_1a_2 - b_1b_2 - c_1c_2 - d_1d_2) + (a_1b_2 + b_1a_2 + c_1d_2 - d_1c_2)\mathbf{i} \\ + (a_1c_2 - b_1d_2 + c_1a_2 + d_1b_2)\mathbf{j} + (a_1d_2 + b_1c_2 - c_1b_2 + d_1a_2)\mathbf{k} \quad (4)$$

which results in another Quaternion. Multiplying Quaternion, Q_2 , by another Q_1 , has the effect of scaling Q_1 by the magnitude of Q_2 followed by a special type of rotation in four dimensions. As such, we can also rewrite the above equation as follows:

$$Q_1 \otimes Q_2 = Q_1 \otimes |Q_2| \left(\frac{Q_2}{|Q_2|} \right) \quad (5)$$

3.2 Quaternion Representations for Knowledge Graph Embedding

Suppose that we have a knowledge graph \mathcal{G} consisting of N entities and M relations. Let \mathcal{R} and \mathcal{E} denote the entities and relations sets in the knowledge graph \mathcal{G} . The training set consists of triplets (h, r, t) with each triplet composed of two entities $h, t \in \mathcal{E}$ and a relationship $r \in \mathcal{R}$. We use Ω to denote the set of observed triples and $\Omega' = \mathcal{E} \times \mathcal{R} \times \mathcal{E} - \Omega$ to denote the set of non-existing triples. $Y_{hrt} \in \{-1, 1\}$ denotes the label of the triple (h, r, t) . The goal is to embed entities and relations to a continuous low-dimensional space, while preserving relevant graph relations and properties. In

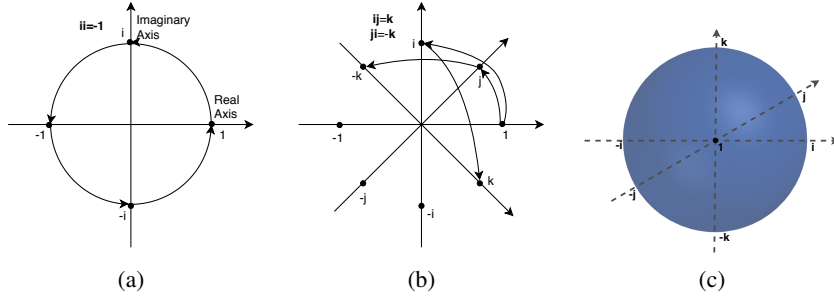


Figure 1: Graphical representation of (a) Complex plane, (b) Quaternion units product and (c) stereographically projected hypersphere in 3D.

the following, we are interested in learning effective representations for entities and relations with Quaternions.

As we mentioned, Quaternions multiplication can be used to represent orientation and rotations in geometry. To get the physical meaning, we can interpret Quaternions to an approximate axis angle representation as follows: $Q = \cos \frac{\theta}{2} + x \sin \frac{\theta}{2} \mathbf{i} + y \sin \frac{\theta}{2} \mathbf{j} + z \sin \frac{\theta}{2} \mathbf{k}$, where θ represents the angle of rotation and x, y, z represent the axis of rotation. Compared to Euler angles, Quaternion can avoid the problem of gimbal lock (loss of one degree of freedom). Quaternions are also more efficient and numerically stable than rotation matrices. Its geometric meaning is also more obvious as the rotation axis and angle can be trivially recovered. The above definition needs not be used explicitly but it provides an intuitive description of what the Quaternion represents.

Quaternion Embeddings of Knowledge Graphs In formal, we use Quaternion matrix $Q \in \mathbb{H}^{N \times k}$ to denote the entities embeddings and $W \in \mathbb{H}^{M \times k}$ to denote the relations embeddings where k is the dimension of embedding. Accordingly, the head entity h is associated with Quaternion $Q_h = \{a_h + b_h \mathbf{i} + c_h \mathbf{j} + d_h \mathbf{k} : a_h, b_h, c_h, d_h \in \mathbb{R}^k\}$ and the tail entity t is associated with Quaternion $Q_t = \{a_t + b_t \mathbf{i} + c_t \mathbf{j} + d_t \mathbf{k} : a_t, b_t, c_t, d_t \in \mathbb{R}^k\}$. Similarly, relation r is represented with Quaternion $W_r = \{a_r + b_r \mathbf{i} + c_r \mathbf{j} + d_r \mathbf{k} : a_r, b_r, c_r, d_r \in \mathbb{R}^k\}$. The basic idea behind our model is as follows. Firstly, we rotate the head Quaternion with normalized relation Quaternion. Subsequently, we use Quaternion dot product to score each triple in the knowledge graph.

Relational Rotation and Hamilton Product In order to rotate the head entity Quaternion with the relation Quaternion, we firstly normalize the relation Quaternion W_r to a unit Quaternion $W_r^\triangleleft = p + q\mathbf{i} + u\mathbf{j} + v\mathbf{k}$. With the definition of a Quaternion norm, we can get the corresponding unit Quaternion by dividing it by its norm.

$$W_r^\triangleleft(p, q, u, v) = \frac{W_r}{|W_r|} = \frac{a_r + b_r \mathbf{i} + c_r \mathbf{j} + d_r \mathbf{k}}{\sqrt{a_r^2 + b_r^2 + c_r^2 + d_r^2}} \quad (6)$$

By constraining the relation Quaternion to have unit magnitude, it yields a three-dimensional space equivalent to the surface of a hypersphere. Since the magnitude is unity, it corresponds to a hypersphere of unit radius. We then compute the Hamilton product between Q_h and W_r^\triangleleft :

$$Q'_h(a'_h, b'_h, c'_h, d'_h) = Q_h \otimes W_r^\triangleleft = (a_h p - b_h q - c_h u - d_h v) + (a_h q + b_h p + c_h v - d_h u) \mathbf{i} \\ + (a_h u - b_h v + c_h p + d_h q) \mathbf{j} + (a_h v + b_h u - c_h q + d_h p) \mathbf{k} \quad (7)$$

with right-multiplication by a unit Quaternion, a right-isoclinic rotation (a general 4D rotation consists of left- and right-isoclinic rotations) is performed on Quaternion Q_h . We can think of Quaternion Q_h as a point and W_r^\triangleleft as an action. We can also swap Q_h and W_r^\triangleleft and do a left-isoclinic rotation, which does not fundamentally change the geometrical meaning. Since we have normalized the relation Quaternion, the scaling effect has been removed. We will also show the results without normalization in Section 4. Note that each multiplication operation in Equation (7) is the element-wise multiplication between two vectors.

Scoring Function and Loss Next, in order to get a scalar prediction, we apply Quaternion dot product as the scoring function:

$$\phi(h, r, t) = Q'_h \cdot Q_t = a'_h \cdot a_t + b'_h \cdot b_t + c'_h \cdot c_t + d'_h \cdot d_t \quad (8)$$

Table 1: Scoring functions of state-of-the-art knowledge graph embedding models, along with their parameters, time complexity. “ \star ” denotes the circular correlation operation; “ \circ ” denotes Hadmard (or element-wise) product. “ \otimes ” denotes Hamilton product.

Model	Scoring Function	Parameters	\mathcal{O}_{time}
TransE	$\ (Q_h + W_r) - Q_t \ $	$Q_h, W_r, Q_t \in \mathbb{R}^k$	$\mathcal{O}(k)$
HolE	$W_r^T (Q_h \star Q_t)$	$Q_h, W_r, Q_t \in \mathbb{R}^k$	$\mathcal{O}(k \log(k))$
DistMult	$Q_h^T \text{diag}(W_r) Q_t$	$Q_h, W_r, Q_t \in \mathbb{R}^k$	$\mathcal{O}(k)$
ComplEx	$\text{Re}(Q_h^T \text{diag}(W_r) \bar{Q}_t)$	$Q_h, W_r, Q_t \in \mathbb{C}^k$	$\mathcal{O}(k)$
RotatE	$\ Q_h \circ W_r - Q_t \ $	$Q_h, W_r, Q_t \in \mathbb{C}^k$	$\mathcal{O}(k)$
TorusE	$\min_{(x,y) \in ([Q_h] + [Q_h]) \times [W_r]} \ x - y \ $	$[Q_h], [Q_h], [W_r] \in \mathbb{T}^k$	$\mathcal{O}(k)$
QuatE	$Q_h \otimes W_r^\triangleleft \cdot Q_t$	$Q_h, W_r, Q_t \in \mathbb{H}^k$	$\mathcal{O}(k)$

Following [Trouillon et al., 2016], we treat the training objective as a classification task and learn the model parameters by minimizing the following regularized logistic loss:

$$L(Q, W) = \sum_{r(h,t) \in \Omega \cup \Omega^-} \log(1 + \exp(-Y_{hrt} \phi(h, r, t))) + \lambda_1 \| Q \|_2^2 + \lambda_2 \| W \|_2^2 \quad (9)$$

Here, we use ℓ_2 norm with regularization rate λ_1 and λ_2 to regularize the model parameters. Ω^- is sampled from the non-observed set Ω' . For simplicity, uniform negative sampling strategy is used. We adopt the adaptive gradient method (Adagrad) [Duchi et al., 2011] to train our model as it can automatically adapt the step size during learning procedure. Note that our loss function is in real space since we take the summation of all components when computing the scoring function in Equation (8).

Initialization Proper initialization may influence the model efficiency and convergence [Glorot and Bengio, 2010]. Here, we adopt the initialization algorithm in [Parcollet et al., 2018b] that is tailored for Quaternion-valued networks. The initialization of entities and relations follows the rule:

$$w_{real} = \varphi \cos(\theta), w_i = \varphi Q_{img_i}^\triangleleft \sin(\theta), w_j = \varphi Q_{img_j}^\triangleleft \sin(\theta), w_k = \varphi Q_{img_k}^\triangleleft \sin(\theta) \quad (10)$$

where w_{real}, w_i, w_j, w_k denote the real and imaginary coefficients of the Quaternion we want to initialize; θ is randomly generated in the interval $[-\pi, \pi]$ and Q_{img}^\triangleleft is a normalized pure Quaternion (the real part equals zero). φ is randomly generated in the interval $[-\frac{1}{\sqrt{2k}}, \frac{1}{\sqrt{2k}}]$, corresponding to the He initialization [He et al., 2015].

3.3 Discussion

Table 1 summarizes several popular knowledge graph embedding models in the literature with their scoring functions, parameters and time complexities. Among all the listed models, TransE, HolE and DistMult use real number embeddings. ComplEx and RotatE operate in complex space while Our model operates in the Quaternion space.

Capability in Modeling Symmetry, Antisymmetry and Inversion. The flexibility and representativeness of Quaternions make it easy to model the major relation patterns for knowledge graph embedding. Similar to ComplEx, our model can model both symmetry ($r(x, y) \Rightarrow r(y, x)$) and antisymmetry ($r(x, y) \Rightarrow \neg r(y, x)$) relations. ComplEx captures the antisymmetry with the Hermitian product while QuatE achieves this with Quaternion Hamilton products. We can check the symmetry property of QuatE by setting the imaginary parts of W_r to zero. The proof of antisymmetry can be found in the Appendix. As for the inversion pattern ($r_1(x, y) \Rightarrow r_2(y, x)$), we can utilize the conjugation of Quaternions. Conjugation is an involution and is its own inverse. Thus, we have:

$$Q_h \otimes W_r^\triangleleft \cdot Q_t = Q_t \otimes \bar{W}_r^\triangleleft \cdot Q_h \quad (11)$$

As for the composition patterns, both transE and RotatE have fixed composition methods. TransE composes two relations with addition ($r_1 + r_2$) and RotatE uses Hadamard product ($r_1 \circ r_2$). We

Table 2: Statistics of the data sets used in this paper.

Dataset	N	M	#training	#validation	#test	#degree
WN18[Bordes et al., 2013]	40943	18	141442	5000	5000	3.45
WN18RR[Detmeters et al., 2018]	40943	11	86835	3034	3134	2.19
FB15K[Bordes et al., 2013]	14951	1345	483142	50000	59071	32.31
FB15K-237[Toutanova and Chen, 2015]	14541	237	272115	17535	20466	18.71

think that it is unreasonable to fix the composition patterns as there might be multiple composition patterns in a knowledge graph².

Connection to DistMult and ComplEx. Quaternions have more degrees of freedom than and subsume complex numbers. Here, we show that how the QuatE framework can degenerate to ComplEx. If we set the coefficients of the imaginary units \mathbf{j} , \mathbf{k} to zero, we get complex embeddings. Then, we remove the normalization of relation Quaternion. We arrive at the following equation:

$$\begin{aligned}
\phi(h, r, t) &= Q_h \otimes W_r \cdot Q_t = (a_h + b_h \mathbf{i}) \otimes (a_r + b_r \mathbf{i}) \cdot (a_t + b_t \mathbf{i}) \\
&= [(a_h a_r - b_h b_r) + (a_h b_r + b_h a_r) \mathbf{i}] \cdot (a_t + b_t \mathbf{i}) \quad (12) \\
&= a_r a_h a_t + a_r b_h b_t + b_r a_h b_t - b_r b_h a_t
\end{aligned}$$

we can see that it recovers the exact form of ComplEx scoring method. This framework also endorses better mathematical interpretation for ComplEx instead of just taking the real part of the Hermitian product. An interesting finding is that Hermitian product is not necessary for ComplEx.

Additionally, if we remove the imaginary parts of all Quaternions and remove the normalization step, the scoring function becomes $\phi(h, r, t) = a_h a_r a_t$. It is obvious that QuatE degrades to DistMult in this case.

4 Experiments and Results

4.1 Experimental Setup

Datasets Description: In order to evaluate our proposal, we conducted experiments on four widely used benchmark datasets WN18, FB15K, WN18RR and FB15K-237. Statistics of them are summarized in Table 2. WN18 [Bordes et al., 2013] is extracted from WordNet³, a lexical database for English language, where words are interlinked by means of conceptual-semantic and lexical relations. WN18RR [Detmeters et al., 2018] is a subset of WN18 which removed inverse relations. FB15K [Bordes et al., 2013] is a large tuple database with structured general human knowledge which includes a diverse of topics. FB15K-237 [Toutanova and Chen, 2015] is a subset of FB15k with inverse relations removed.

Evaluation Protocol: Three popular evaluation metrics are used in this experiment including: Mean Rank(MR), Mean Reciprocal Rank (MRR) and Hit ratio with given cut-off value n (1, 3, 10). MR measures the average rank of all correct entities with lower value representing better performance. MRR is the average inverse rank for correct entities. Hit@ n measures the proportion of correct entities in the top n entities. Same as [Bordes et al., 2013], filtered results are reported to avoid possibly flawed evaluation.

Baselines: We compared QuatE with a number of recent baselines in the literature. For (1) *Translational Distance Models*, we reported the most representative translational method - TransE [Bordes et al., 2013], and two recent extensions TorusE [Ebisu and Ichise, 2018] and RotatE [Sun et al., 2019]; For (2) *Semantic Matching Models*, we reported DistMult [Yang et al., 2014], HolE [Nickel et al., 2016], ComplEx [Trouillon et al., 2016], Simple [Kazemi and Poole, 2018], ConvE [Detmeters et al., 2018], R-GCN [Schlichtkrull et al., 2018] and KNGE (ConvE based) [Wang et al., 2018].

Implementation Details: We implement our model by following the open-source toolkit OpenKE [Han et al., 2018], and test it on a single GPU. We determine the hyper-parameters by grid

²We can give a simple example that violates the two composition methods of TransE and RotatE: suppose we have three person “ x, y, z ”, if y is the elder sister (denotes as r_1) of x and z is the elder brother (denotes as r_2) of y ; we can easily infer that z is the elder brother (equals to r_2 instead of $r_1 + r_2$ or $r_1 \circ r_2$) of x .

³<https://wordnet.princeton.edu/>

Table 3: Link prediction results on WN18 and FB15K. Best results are in bold and second best results are underlined. [†]: Results are taken from [Nickel et al., 2016]; [◇]: Results are taken from [Kadlec et al., 2017].

Model	WN18					FB15K				
	MR	MRR	Hit@10	Hit@3	Hit@1	MR	MRR	Hit@10	Hit@3	Hit@1
TransE†	-	0.495	0.943	0.888	0.113	-	0.463	0.749	0.578	0.297
DistMult◇	655	0.797	0.946	-	-	42.2	0.798	<u>0.893</u>	-	-
HolE	-	0.938	0.949	0.945	0.930	-	0.524	0.739	0.759	0.599
ComplEx	-	0.941	0.947	0.945	0.936	-	0.692	0.840	0.759	0.599
ConvE	374	0.943	0.956	0.946	0.935	51	0.657	0.831	0.723	0.558
R-GCN+	-	0.819	0.964	0.929	0.697	-	0.696	0.842	0.760	0.601
Simple	-	0.942	0.947	0.944	0.939	-	0.727	0.838	0.773	0.660
NKGE	336	<u>0.947</u>	0.957	0.949	0.942	56	0.73	0.871	<u>0.790</u>	0.650
TorusE	-	<u>0.947</u>	0.954	0.950	<u>0.943</u>	-	0.733	0.832	<u>0.771</u>	<u>0.674</u>
RotatE	<u>184</u>	<u>0.947</u>	<u>0.961</u>	<u>0.953</u>	0.938	<u>32</u>	0.699	0.872	0.788	0.585
QuatE	162	0.950	0.959	0.954	0.945	17	<u>0.782</u>	0.900	0.835	0.711

Table 4: Link prediction results on WN18RR and FB15K-237. [†]: Results are taken from [Nguyen et al., 2017]; [◇]: Results are taken from [Dettmers et al., 2018]; [*]: Results on FB15K-237 are taken from [Sun et al., 2019].

Model	WN18RR					FB15K-237				
	MR	MRR	Hit@10	Hit@3	Hit@1	MR	MRR	Hit@10	Hit@3	Hit@1
TransE †	3384	0.226	0.501	-	-	357	0.294	0.465	-	-
DistMult◇	5110	0.43	0.49	0.44	0.39	254	0.241	0.419	0.263	0.155
ComplEx◇	5261	0.44	0.51	0.46	0.41	339	0.247	0.428	0.275	0.158
ConvE◇	4187	0.43	0.52	0.44	0.40	244	0.325	0.501	0.356	0.237
R-GCN+	-	-	-	-	-	-	0.249	0.417	0.264	0.151
NKGE	4170	0.45	0.526	0.465	0.421	237	<u>0.33</u>	<u>0.510</u>	<u>0.365</u>	<u>0.241</u>
RotatE*	<u>3277</u>	<u>0.470</u>	<u>0.564</u>	<u>0.488</u>	<u>0.422</u>	<u>185</u>	0.297	0.480	0.328	0.205
QuatE	2608	0.480	0.567	0.500	0.434	88	0.347	0.546	0.381	0.248

search. Best models are selected by early stopping on the validation set. The embedding size k is tuned amongst $\{50, 100, 200, 250\}$. Regularization rate λ_1 and λ_2 is validated in $\{0, 0.01, 0.05, 0.1, 0.2\}$. Learning rate is fixed to 0.1 without further tuning. The number of negatives ($\#neg$) per training sample is selected from $\{1, 5, 10, 20, 30\}$. We create 10 batches for all datasets. For fair comparison, tricks such as reciprocal relations which adds inverse relations for each triplet [Lacroix et al., 2018, Lerer et al., 2019], self-adversarial negative sampling [Sun et al., 2019], are not used since our focus is to compare the effectiveness of different scoring methods. For most baselines, we report the results in the corresponding published papers, and exceptions are provided with references. For RotatE, we use the best hyper-parameter settings provided in the paper to reproduce the results.

4.2 Results

The empirical results of our proposed model and baselines on four datasets are reported in Table 3 and Table 4. It can be viewed that QuatE performs extremely competitively compared to the existing state-of-the-art models across all metrics. Detailed observations are summarized in the following text.

For the WN18 dataset, QuatE outperforms all the baselines on all metrics except Hit@10. R-GCN+ achieves high value on Hit@10 but are surpassed by most models on the other four metrics. The three recent models NKGE, TorusE and RotaE achieves comparative results; QuatE also achieves the best results on the FB15K dataset, while the second best results are scatters amongst NKGE, TorusE and DistMult. We are well-aware of the good results of DistMult reported in [Kadlec et al., 2017], but we also noticed that they used a very large negative sampling size (i.e., 1000, 2000). We are not able to conduct experiments with this size due to limited computation resources. The results also demonstrate that QuatE can capture the symmetry, antisymmetry and inversion patterns since they account for a large portion of the relationships in these two datasets.

Table 5: Number of free parameters comparison on four datasets.

Model	Space	WN18	FB15K	WN18RR	FB15K-237
TorusE	Torus	409.61M	162.96M	-	-
RotatE	Complex	40.95M	31.25M	40.95M	29.32M
QuatE	Quaternion	40.96M	26.08M	16.38M	5.82M

Table 6: Analysis on different variants of scoring function. Same hyperparameters as QuatE are used.

Analysis	WN18		FB15K		WN18RR		FB15K-237	
	MRR	Hit@10	MRR	Hit@10	MRR	Hit@10	MRR	Hit@10
$Q_h \otimes W_r \cdot Q_t$	0.936	0.951	0.686	0.866	0.415	0.469	0.272	0.463
$W_r \cdot (Q_h \otimes Q_t)$	0.784	0.945	0.599	0.809	0.401	0.471	0.263	0.446
$(Q_h \otimes W_r^{\triangleleft}) \cdot (Q_t \otimes V_r^{\triangleleft})$	0.947	0.958	0.787	0.889	0.477	0.563	0.344	0.539

As shown in Table 4, QuatE achieves a reasonably large performance gain over existing state-of-the-art models on the two datasets where trivial inverse relations are removed. On WN18RR in which there are a number of symmetry relations, RotatE comes in second while other baselines are relatively weaker. The key competitors on dataset FB15K-237 where a large number of composition patterns exist are neural network based approaches NKG E and ConvE. Models with fixed composition patterns like TransE and RotatE perform poorly and surpassed by neural network methods and QuatE.

We also observe an obvious clear margin in the metric Mean Rank that our model achieves considerably lower Mean Rank and even reduce it to half of the second best result on FB15K-237. Evidently, QuatE could rank ground-truth triplets higher on average.

4.3 Model Analysis

Number of Free Parameters Comparison. Table 5 shows the amount of parameters comparison between QuatE and two recent baselines: RotatE and TorusE. TorusE uses a very large embedding dimension 10000 for both WN18 and FB15K. This number is even close to the entities amount of FB15K which we think is not preferable since our original intention is to embed entities and relations to a lower dimensional space. In addition, QuatE reduces the parameter size of the complex-valued counterpart RotatE down to one fourth while maintaining superior performance.

Ablation Study on Quaternion Normalization. We remove the normalization step in QuatE and use the original relation Quaternion W_r to project head entity. From Table 6, we clearly observe that normalizing the relation to unit Quaternion is a critical step for the embedding performance. This is likely because scaling effects in nonunit Quaternions are detrimental.

Hamilton Products between Head and Tail Entities. We reformulate the scoring function of QuatE following the original formulate of ComplEx. We do Hamilton product between head and tail Quaternions and consider the relation Quaternion as weight. Thus, we have $\phi(h, r, t) = W_r \cdot (Q_h \otimes Q_t)$. As a result, the geometric interpretation of relational rotation is lost, which leads to poor performance as shown in Table 6.

Additional Rotational Quaternion for Tail Entity. We hypothesize that adding an additional relation Quaternion to tail entity might bring the model more representation capability. So we revise the scoring function to $(Q_h \otimes W_r^{\triangleleft}) \cdot (Q_t \otimes V_r^{\triangleleft})$, where V_r represents the rotational Quaternion for tail entity. From Table 6, we observe that it achieves similar results as QuatE without extensive tuning. However, it might cause some losses of efficiency.

5 Conclusion

In this paper, we design a new knowledge graph embedding model which operates on the Quaternion space with well-defined mathematical and physical meaning. Our model is advantageous with its capability in modelling several key relation patterns, expressiveness with higher degrees of freedom as well as its good generalization. Empirical experimental evaluations on four well-established datasets show that QuatE achieves an overall state-of-the-art performance, outperforming multiple recent strong baselines, with even fewer free parameters.

References

- Antoine Bordes, Nicolas Usunier, Alberto Garcia-Duran, Jason Weston, and Oksana Yakhnenko. Translating embeddings for modeling multi-relational data. In *Advances in neural information processing systems*, pages 2787–2795, 2013.
- Tim Dettmers, Pasquale Minervini, Pontus Stenetorp, and Sebastian Riedel. Convolutional 2d knowledge graph embeddings. In *Thirty-Second AAAI Conference on Artificial Intelligence*, 2018.
- Xin Dong, Evgeniy Gabrilovich, Jeremy Heitz, Wilko Horn, Ni Lao, Kevin Murphy, Thomas Strohmann, Shaohua Sun, and Wei Zhang. Knowledge vault: A web-scale approach to probabilistic knowledge fusion. In *Proceedings of the 20th ACM SIGKDD international conference on Knowledge discovery and data mining*, pages 601–610. ACM, 2014.
- John Duchi, Elad Hazan, and Yoram Singer. Adaptive subgradient methods for online learning and stochastic optimization. *Journal of Machine Learning Research*, 12(Jul):2121–2159, 2011.
- Takuma Ebisu and Ryutaro Ichise. Toruse: Knowledge graph embedding on a lie group. In *Thirty-Second AAAI Conference on Artificial Intelligence*, 2018.
- Chase J Gaudet and Anthony S Maida. Deep quaternion networks. In *2018 International Joint Conference on Neural Networks (IJCNN)*, pages 1–8. IEEE, 2018.
- Xavier Glorot and Yoshua Bengio. Understanding the difficulty of training deep feedforward neural networks. In *Proceedings of the thirteenth international conference on artificial intelligence and statistics*, pages 249–256, 2010.
- William Rowan Hamilton. Lxxviii. on quaternions; or on a new system of imaginaries in algebra: To the editors of the philosophical magazine and journal. *The London, Edinburgh, and Dublin Philosophical Magazine and Journal of Science*, 25(169):489–495, 1844.
- Xu Han, Shulin Cao, Lv Xin, Yankai Lin, Zhiyuan Liu, Maosong Sun, and Juanzi Li. Openke: An open toolkit for knowledge embedding. In *Proceedings of EMNLP*, 2018.
- Kaiming He, Xiangyu Zhang, Shaoqing Ren, and Jian Sun. Delving deep into rectifiers: Surpassing human-level performance on imagenet classification. In *Proceedings of the IEEE international conference on computer vision*, pages 1026–1034, 2015.
- Guoliang Ji, Shizhu He, Liheng Xu, Kang Liu, and Jun Zhao. Knowledge graph embedding via dynamic mapping matrix. In *Proceedings of the 53rd Annual Meeting of the Association for Computational Linguistics and the 7th International Joint Conference on Natural Language Processing (Volume 1: Long Papers)*, volume 1, pages 687–696, 2015.
- Rudolf Kadlec, Ondrej Bajgar, and Jan Kleindienst. Knowledge base completion: Baselines strike back. *ACL 2017*, page 69, 2017.
- Seyed Mehran Kazemi and David Poole. Simple embedding for link prediction in knowledge graphs. In *Advances in Neural Information Processing Systems*, pages 4289–4300, 2018.
- Timothee Lacroix, Nicolas Usunier, and Guillaume Obozinski. Canonical tensor decomposition for knowledge base completion. In *International Conference on Machine Learning*, pages 2869–2878, 2018.
- Adam Lerer, Ledell Wu, Jiajun Shen, Timothee Lacroix, Luca Wehrstedt, Abhijit Bose, and Alex Peysakhovich. PyTorch-BigGraph: A Large-scale Graph Embedding System. In *Proceedings of the 2nd SysML Conference*, Palo Alto, CA, USA, 2019.
- Yankai Lin, Zhiyuan Liu, Maosong Sun, Yang Liu, and Xuan Zhu. Learning entity and relation embeddings for knowledge graph completion. In *Twenty-ninth AAAI conference on artificial intelligence*, 2015.
- Dai Quoc Nguyen, Tu Dinh Nguyen, Dat Quoc Nguyen, and Dinh Phung. A novel embedding model for knowledge base completion based on convolutional neural network. *arXiv preprint arXiv:1712.02121*, 2017.

- Maximilian Nickel, Volker Tresp, and Hans-Peter Kriegel. A three-way model for collective learning on multi-relational data. In *ICML*, volume 11, pages 809–816, 2011.
- Maximilian Nickel, Lorenzo Rosasco, and Tomaso Poggio. Holographic embeddings of knowledge graphs. In *Thirtieth Aaai conference on artificial intelligence*, 2016.
- T. Parcollet, M. Morchid, P. Bousquet, R. Dufour, G. Linares, and R. De Mori. Quaternion neural networks for spoken language understanding. In *2016 IEEE Spoken Language Technology Workshop (SLT)*, pages 362–368, Dec 2016. doi: 10.1109/SLT.2016.7846290.
- Titouan Parcollet, Ying Zhang, Mohamed Morchid, Chiheb Trabelsi, Georges Linares, Renato De Mori, and Yoshua Bengio. Quaternion convolutional neural networks for end-to-end automatic speech recognition. *arXiv preprint arXiv:1806.07789*.
- Titouan Parcollet, Mohamed Morchid, and Georges Linares. Quaternion denoising encoder-decoder for theme identification of telephone conversations. In *INTERSPEECH*, 2017.
- Titouan Parcollet, Mohamed Morchid, and Georges Linares. Quaternion convolutional neural networks for heterogeneous image processing. *CoRR*, abs/1811.02656, 2018a. URL <http://arxiv.org/abs/1811.02656>.
- Titouan Parcollet, Mirco Ravanelli, Mohamed Morchid, Georges Linares, Chiheb Trabelsi, Renato De Mori, and Yoshua Bengio. Quaternion recurrent neural networks. *The International Conference on Learning Representations*, abs/1806.04418, 2018b.
- Sara Sabour, Nicholas Frosst, and Geoffrey E Hinton. Dynamic routing between capsules. In *Advances in neural information processing systems*, pages 3856–3866, 2017.
- Michael Schlichtkrull, Thomas N Kipf, Peter Bloem, Rianne Van Den Berg, Ivan Titov, and Max Welling. Modeling relational data with graph convolutional networks. In *European Semantic Web Conference*, pages 593–607. Springer, 2018.
- Richard Socher, Danqi Chen, Christopher D Manning, and Andrew Ng. Reasoning with neural tensor networks for knowledge base completion. In *Advances in neural information processing systems*, pages 926–934, 2013.
- Zhiqing Sun, Zhi-Hong Deng, Jian-Yun Nie, and Jian Tang. Rotate: Knowledge graph embedding by relational rotation in complex space. 2019.
- Kristina Toutanova and Danqi Chen. Observed versus latent features for knowledge base and text inference. In *Proceedings of the 3rd Workshop on Continuous Vector Space Models and their Compositionality*, pages 57–66, 2015.
- Théo Trouillon and Maximilian Nickel. Complex and holographic embeddings of knowledge graphs: a comparison. *arXiv preprint arXiv:1707.01475*, 2017.
- Théo Trouillon, Johannes Welbl, Sebastian Riedel, Éric Gaussier, and Guillaume Bouchard. Complex embeddings for simple link prediction. In *International Conference on Machine Learning*, pages 2071–2080, 2016.
- Kai Wang, Yu Liu, Xiujuan Xu, and Dan Lin. Knowledge graph embedding with entity neighbors and deep memory network. *arXiv preprint arXiv:1808.03752*, 2018.
- Zhen Wang, Jianwen Zhang, Jianlin Feng, and Zheng Chen. Knowledge graph embedding by translating on hyperplanes. In *Twenty-Eighth AAAI conference on artificial intelligence*, 2014.
- Bishan Yang, Wen-tau Yih, Xiaodong He, Jianfeng Gao, and Li Deng. Embedding entities and relations for learning and inference in knowledge bases. *arXiv preprint arXiv:1412.6575*, 2014.

6 Appendix

6.1 Proof of Antisymmetry

In order to prove the antisymmetry pattern, we need to prove that:

$$Q_h \otimes W_r^\triangleleft \cdot Q_t \neq Q_t \otimes W_r^\triangleleft \cdot Q_h \quad (13)$$

Firstly, we expand the left term:

$$\begin{aligned} Q_h \otimes W_r^\triangleleft \cdot Q_t &= [(a_h p - b_h q - c_h u - d_h v) + (a_h q + b_h p + c_h v - d_h u)\mathbf{i} + \\ &\quad (a_h u - b_h v + c_h p + d_h q)\mathbf{j} + (a_h v + b_h u - c_h q + d_h p)\mathbf{k}] \cdot \\ &\quad (a_t + b_t \mathbf{i} + c_t \mathbf{j} + d_t \mathbf{k}) \\ &= (a_h p - b_h q - c_h u - d_h v)a_t + (a_h q + b_h p + c_h v - d_h u)b_t + \\ &\quad (a_h u - b_h v + c_h p + d_h q)c_t + (a_h v + b_h u - c_h q + d_h p)d_t \\ &= a_h p a_t - b_h q a_t - c_h u a_t - d_h v a_t + a_h q b_t + b_h p b_t + c_h v b_t - d_h u b_t + \\ &\quad a_h u c_t - b_h v c_t + c_h p c_t + d_h q c_t + a_h v d_t + b_h u d_t - c_h q d_t + d_h p d_t \end{aligned} \quad (14)$$

We then expand the right term:

$$\begin{aligned} Q_t \otimes W_r^\triangleleft \cdot Q_h &= [(a_t p - b_t q - c_t u - d_t v) + (a_t q + b_t p + c_t v - d_t u)\mathbf{i} + \\ &\quad (a_t u - b_t v + c_t p + d_t q)\mathbf{j} + (a_t v + b_t u - c_t q + d_t p)\mathbf{k}] \cdot \\ &\quad (a_h + b_h \mathbf{i} + c_h \mathbf{j} + d_h \mathbf{k}) \\ &= (a_t p - b_t q - c_t u - d_t v)a_h + (a_t q + b_t p + c_t v - d_t u)b_h + \\ &\quad (a_t u - b_t v + c_t p + d_t q)c_h + (a_t v + b_t u - c_t q + d_t p)d_h \\ &= a_t p a_h - b_t q a_h - c_t u a_h - d_t v a_h + a_t q b_h + b_t p b_h + c_t v b_h - d_t u b_h + \\ &\quad a_t u c_h - b_t v c_h + c_t p c_h + d_t q c_h + a_t v d_h + b_t u d_h - c_t q d_h + d_t p d_h \end{aligned} \quad (15)$$

We can easily see that those two terms are not equal as the signs for some terms are not the same. The same case also holds for equation 12.

6.2 Hyperparameters Settings

We list the best hyperparameters setting of QuatE on the benchmark datasets:

- WN18: $k = 250, \lambda_1 = 0.05, \lambda_2 = 0, \#neg = 10$
- FB15K: $k = 200, \lambda_1 = 0.1, \lambda_2 = 0, \#neg = 20$
- WN18RR: $k = 100, \lambda_1 = 0.03, \lambda_2 = 0.03, \#neg = 1$
- FB15K-237: $k = 100, \lambda_1 = 0.2, \lambda_2 = 0.2, \#neg = 1$